



Observations and modelling of mosquito prevalence within urban areas – A case study from Uppsala, Sweden

Fredrik Lindberg¹ · Anders Lindström² · Ville Stålnacke^{1,3} · Sofia Thorsson¹ · Georgia Destouni^{4,5}

Accepted: 14 January 2024
© The Author(s) 2024

Abstract

Urban green–blue infrastructure (GBI) can provide important benefits to urban residents but may also affect mosquito abundance, with associated negative nuisance and infection transmission impacts. This study addresses important knowledge and quantification gaps for the relationships between mosquito prevalence and GBI features within cities. This is done for the city of Uppsala in Sweden as an urban case example, where mosquitoes were captured and ambient air temperature and humidity were observed at seven different locations in the summer of 2022. A weighted multi-criteria analysis (WMCA) model was developed based on relevant open data and open tools for resolving the mosquito (*Culex pipiens*) variations based on geographical variables, such as land cover/use, leaf area index, and building and green (vegetation) area fractions, within the city. The results show a clear relationship between mosquito prevalence and green-area fraction (of grass and trees), indicating that urban GBI extension can enhance mosquito prevalence, with possible associated negative impacts. This relationship is supported directly by data, showing significantly higher mosquito prevalence with higher ambient humidity, which in turn is related to larger green-area fraction. The developed WMCA model emerges as a promising tool, e.g., for urban development planning that needs to account for and seek relevant trade-off balances between positive and negative effects of urban GBI changes.

Keywords Geographical information system · Green–blue infrastructure · Urban warming · *Culex pipiens*

Introduction

There is increasing awareness that urban green–blue infrastructure (GBI; areas of natural, restored, or (re)constructed ecosystems, e.g., forested land, wetlands, parks) can provide a range of benefits to the urban residents, such as reduce risk of flooding and mitigate heat stress (Goldenberg et al. 2017, 2021; Konarska et al. 2016), and improve resident health,

physical activity, and overall wellbeing (Goldenberg et al. 2018). However, there is also risk for adverse GBI effects on humans, for example due to enhanced breeding grounds for mosquitoes that may cause nuisance and transmit infectious diseases (Ma et al. 2019, 2020).

Mosquitoes need water and vegetation to be able to breed and thrive. Several common and widespread mosquito species, such as *Culex (Cx.) pipiens*, *Cx. torrentium*, *Aedes (Ae.) geniculatus*, *Coquillettidia (Cq.) richiardii*, *Culiseta (Cs.) annulata* and *Anopheles (An.) plumbeus*, breed continuously through the summer and can often be found in urban areas (Krüger et al. 2014; Lundström et al. 2013). Some of these are potential disease vectors, for example for West Nile virus and Usutu virus causing encephalitis, Sindbis virus and Chikungunya virus, and the bacterium *Francisella tularensis* causing tularemia. In a warmer climate, which is also exacerbated by the urban warming effect, there is a considerable risk for northward spread of invasive urban mosquito species that are currently established in more southern parts of Europe, such as *Aedes japonicus*, *Aedes koreicus* and *Aedes albopictus* (Medlock

✉ Fredrik Lindberg
fredrikl@gvc.gu.se

¹ Department of Earth Sciences, University of Gothenburg, Gothenburg, Sweden

² National Veterinary Institute, Uppsala, Sweden

³ WSP Sweden, Östersund, Sweden

⁴ Department of Physical Geography, Stockholm University, Stockholm, Sweden

⁵ Department of Sustainable Development, Environmental Science and Engineering, KTH Royal Institute of Technology, Stockholm, Sweden

et al. 2012). The presence of *Ae. albopictus* in Europe have caused autochthonous outbreaks of diseases such as Dengue, chikungunya and zika (Jourdain et al. 2020). Mosquitoes of the *Cx. pipiens/torrentium* complex are often regarded as drivers of WNV outbreaks in Europe (Engler et al. 2013). Larger populations of these species correspond to a higher risk of outbreaks (Kramer and Ciota 2015). They share similar biological traits; overwintering as adult females, breeding continuously through summer in almost any kind of water collections resulting in large populations at the end of summer and being ornithophilic (Becker et al. 2020).

Increased populations of vector species are a risk factor per se for enhanced pathogen transmission (Kramer and Ciota 2015; Ma et al. 2019). A warmer climate may lead to shorter generation times and longer reproductive seasons, leading to larger mosquito populations and an escalated risk for transmission of mosquito borne infections in and around urban heat islands (Paz and Albersheim 2008). For example, the Nordic climate is currently considered too cold for virus-pathogens such as the West Nile virus to develop, and no outbreaks have occurred in Scandinavia (Public Health Agency of Sweden 2019). With a warming climate, however, the virus can spread to higher latitudes (Petrić et al. 2017), especially during summer heat waves as indicated by recent outbreaks of West Nile fever in Germany and Netherlands (Frank et al. 2022; Vlaskamp et al. 2020). Moreover, not just temperature increase, but also water-related increases in precipitation, stream/river flows and associated water inundation events at relevant times of the year can enhance mosquito abundance and related spreading of infections (Ma et al. 2019, 2020).

Urban constructions can both counteract and exacerbate the emergence of disease environments related to GBI, depending on how the disease factors are accounted for in the design and construction stages. For instance, an increase in wet areas is a risk because the density of larval populations in such areas exceeds those in other, drier environments. Studies have shown that wet environments and wetlands are dominant mosquito producers in urban regions, e.g., in Sweden (Åhlen et al. 2023). Other studies have shown the importance of water in urban parks for increased incidence of disease-bearing mosquitoes in Brazil as well as in Sweden (Desvars et al. 2015). Furthermore, studies in both USA and Europe have reported positive associations between mosquito presence, abundance and diversity and NDVI, an index of photosynthetic activity (Diuk-Wasser et al. 2006; Ferraguti et al. 2016; Reisen et al. 1990; Roiz et al. 2015). That is, higher values of NDVI reflect a greater vegetation cover that may increase resting habitats for mosquitoes.

Current knowledge of the spatial distribution of mosquitoes within cities and the factors affecting it is limited and requires further research. Krüger et al. (2014)

studied the mosquito fauna of metropolitan Hamburg and found that mosquitoes of the *pipiens*-complex were the most common. They used the Corine Land Cover Classification (www.eea.europa.eu), lumping all urban land-cover categories into one urban class, and considering also three “non-urban” classes (Krüger et al. 2014). Using the same land cover source for an inventory of the mosquitoes in Belgium, Verstiart et al. (2013) report the species found in urban areas, showing these to be the least species-rich environment in Belgium, without further analysis of mosquito variations within the urban areas. An inventory of *Cx. pipiens* and *Cx. torrentium* over Germany also does not report variations within the urban areas (Rudolf et al. 2013). Models for mosquito prevalence exist on a regional scale (e.g., Krol et al. 2023) but, to the best of our knowledge, without sufficient spatial resolution and urban domain focus for resolving variations within urban areas.

This paper addresses the knowledge and modelling gaps of spatio-temporal mosquito variations within urban areas under various urban GBI conditions. This is done for the city of Uppsala in Sweden as an urban case example, where mosquitos were captured and ambient air temperature and humidity data were collected at seven different locations in the summer of 2022. A WMCA-based (Weighted Multi-Criteria Analysis) GIS model named Urban Mosquito Prevalence (UMP) was also developed based on relevant open data and tools for resolving and quantifying the mosquito prevalence relationships with GBI features within this Swedish case example. Such resolution and quantification are generally needed, e.g., for urban development planning that needs to account for and seek relevant trade-off balances between positive and potential negative GBI effects.

Methods

Observations

Field observations of mosquito prevalence, ambient air temperature and humidity were conducted during the summer of 2022 (June 1st to September 15th) in Uppsala, Sweden. Seven different locations were chosen based on variations in land use and urban density (Fig. 1 and Table 1).

Air temperature and humidity were retrieved by Tinytag Plus2 Dataloggers (TPG-4500) at 10-min intervals, 3 m above ground encapsulated in tube radiation shields. The Tinytag logger for the Mixed city location went missing and only observations from the mosquito trap are available from that location for the present analysis. General meteorological parameters (air temperature, humidity, pressure, precipitation) was also retrieved from the official meteorological station (station number: 97510) maintained by the Swedish Meteorological and Hydrological Institute (SMHI). BG

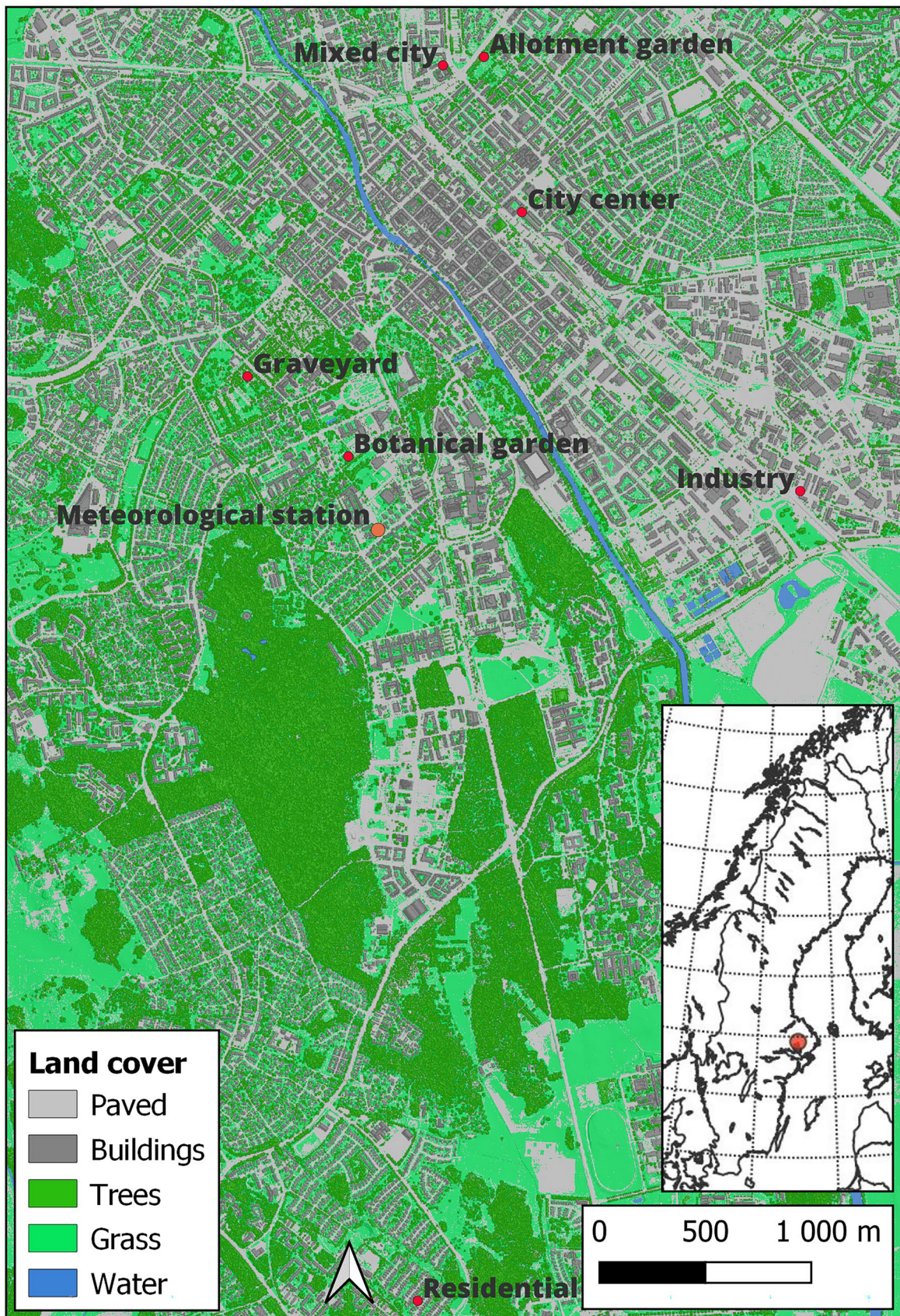


Fig. 1 Overview map of study area and mosquito capture locations point in Uppsala, Sweden

Table 1 Fractions and heights of buildings and vegetation derived from a 100-m radius around each site location

Site location	Building fraction	Mean building height	Green fraction	Mean tree height
Allotment garden	0.08	8.7	0.56	9.8
Mixed city	0.25	14.6	0.18	11.9
City centre	0.33	14.6	0.16	9.6
Graveyard	0.01	4.3	0.62	12.7
Botanical garden	0.03	7.8	0.63	7.9
Industry	0.24	6.2	0.06	7.0
Residential	0.31	4.8	0.45	6.9

Sentinel traps with CO₂ and without the lure were used. The traps were set every two weeks and ran for approximately 24 h. The trapped mosquitoes were put in a freezer within two hours of emptying the traps. Mosquito identification was done with the keys in Lindström and Eklöf (2022). To differentiate between *Cx. pipiens* and *Cx. torrentium* we used the protocol for real-time PCR described in Vogels et al. (2015).

Model description

The UMP-model (Urban Mosquito Prevalence) is a further development of the work by Stålnacke (2021). The model is a WMCA-based GIS model and is primarily designed for implementation using Swedish national geodata, but can easily be adapted for and applied to urban areas in other countries with similar data availability.

A simplified workflow of the modelling process is shown in Fig. 2. The UMP-model is written in Python programming language and exploits the PyQGIS API (QGIS.org 2023) to prepare, manage, and reclassify the datasets that were used as inputs in the WMCA sections of the models. FUSION LDV (McGaughey 2009) has been used for all LiDAR-processing. All parts of the model and the LiDAR data preparation code are available from (Lindberg and Stålnacke 2023) with the repository links also given in the Data availability section.

Geodata

The datasets used in the model are presented in Table 2. The ambition of the data collection was to exploit data with a full Swedish national coverage, as one ambition of the models developed is the possibility to directly implement them in other cities in Sweden. Three datasets were used for fine scale building-, ground- and vegetation heights, namely a Digital Surface Model (DSM), a Digital Elevation Model (DEM) and a Canopy Digital Surface Model (CDSM) (Lindberg and Grimmond 2011). These datasets are derived from national LiDAR-data produced by the Swedish Mapping Cadastral and Land Registration Authority (Lantmäteriet) and gridded at 2-m resolution (Lantmäteriet 2023). The Leaf Area Index (LAI)-dataset at 10-m resolution is also derived from the same LiDAR-data according to Klingberg et al. (2017). The national land cover datasets from the Swedish Environmental Protection Agency (Naturvårdsverket) were used for high resolution raster data of land cover, land use and object heights. In Swedish, the datasets are called Nationella Marktäckesdatan, (NMD). The mapping for the NMD-data was performed 2017–2019, and the plan is to update the mapping every five years (Swedish Environmental Protection Agency 2020). Two vector datasets were used, one building dataset and one land use dataset, to locate buildings and other land uses of relevance. Both were collected from Lantmäteriet (2021).

IUHI-model

A simple Intra Urban Heat Island (IUHI) sub-model was developed to identify areas where oviposition sites are more favorable. The model used the inputs of DSM, DEM and CDSM as well as a within-model created vector-grid to calculate IUHI from the warming effect of the building density and the cooling effect from vegetation.

Oke (2002) proposed a relationship between building's height to street's width (H/W-ratio) and maximum urban heat island intensity, $\Delta T_{u-r(max)}$ during prime weather conditions (clear and calm) to be (Eq. 1):

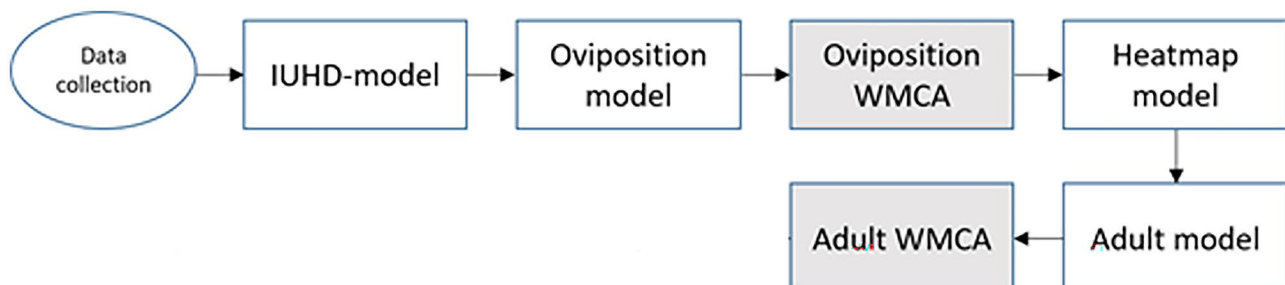


Fig. 2 A simplified version of the workflow utilized for the Urban Mosquito Prevalence (UMP) model presented in this paper. White boxes indicate sub-models. Grey boxes indicate model results. IUHI = Intra Urban Heat Island, WMCA = Weighted Multi-Criteria Analysis

Table 2 Datatype, pixel size, supplier, coverage, and model of use of the datasets utilized in the study

Data	Pixel size (m)	Supplier/Processing	Model of use
Digital Surface Model (DSM) [R]	2	Generated from Point cloud (Lantmäteriet)	Intra Urban Heat Island, Oviposition
Digital Elevation Model (DEM) [R]	2	Generated from Point cloud (Lantmäteriet)	Intra Urban Heat Island, Adult
Canopy Digital Surface Model (CDSM) [R]	2	Generated from Point cloud (Lantmäteriet)	Intra Urban Heat Island
NMD Land Cover [R]	10	Swedish Environmental Protection Agency (Naturvårdsverket)	Oviposition, Adult
NMD Land Use [R]	10	Swedish Environmental Protection Agency (Naturvårdsverket)	Oviposition
NMD Object Heights 0.5–5 m [R]	10	Swedish Environmental Protection Agency (Naturvårdsverket)	Adult
NMD Object Heights 5–45 m [R]	10	Swedish Environmental Protection Agency (Naturvårdsverket)	Adult
Buildings [V]	NA	Swedish Mapping, Cadastral and Land Registration Authority (Lantmäteriet)	Oviposition
Land Use Vector [V]	NA	Swedish Mapping, Cadastral and Land Registration Authority (Lantmäteriet)	Oviposition, Adult
Leaf Area Index (LAI) [R]	2	Generated from Point cloud (Lantmäteriet)	Adult

$$\Delta T_{u-r(\max)} = 7.54 + 3.97 \ln H/W \quad (1)$$

where $\ln(H/W)$ is the natural logarithm of the H/W-ratio. Here, the H/W-ratio was calculated with the following Eq. (2) (Lindberg et al. 2015):

$$H/W = \frac{\lambda_w \lambda_p}{2\lambda_p(1 - \lambda_p)} \quad (2)$$

where λ_w is the wall area fraction and λ_p is the building area fraction (also known as Plan Area Index). The λ_w was defined with the following Eq. (3):

$$\lambda_w = \frac{Area_{wall}}{Area_{road} + Area_{roof}} \quad (3)$$

where $Area_{wall}$ is the wall area, $Area_{road}$ is the road area and $Area_{roof}$ is the roof area (Lindberg et al. 2015). To calculate $Area_{wall}$, the height of walls was needed to be calculated. This was accomplished via an algorithm in the Urban Multi-Scale Environmental Predictor (UMEP)-plugin (Lindberg et al. 2018). The algorithm calculates wall heights for each building, using the DSM as input layer. λ_p was calculated via an UMEP-algorithm which calculates a variety of urban-morphological parameters from digital surface models.

The plan area of vegetation ($\lambda_{p\text{veg}}$) was used to calculate the cooling effect of trees, via the Eq. (4) from Krayenhoff et al. 2021):

$$Tree\ cooling\ effect = 0.3 \left(\frac{\lambda_{p\text{veg}}}{0.1} \right) \quad (4)$$

The tree cooling effect was subtracted from the H/W-warming effect to get the IUHI, via the following equation:

$$IUHI = \frac{H}{W} \text{warming} - \text{Tree cooling effect} \quad (5)$$

Oviposition model

Cx. pipiens are experts at finding oviposition sites in urban areas and they can lay their eggs in a variety of small water containers if they remain undisturbed. Due to the high adaptive capacity of the *Cx. pipiens*, as well as the utilized water containers being smaller-than- microscale, the complexity was hard to grasp via a model. Therefore, a simplified model of oviposition suitability was produced. The model reclassifies land use, land cover and IUHI, depending on their suitability as oviposition sites for *Cx. pipiens*. The input data and their application can be seen in Table 3.

Flat roofs (slope $< 8^\circ$) were identified via the DSM and the vector-dataset of buildings, as oviposition sites can be found on roofs as well. To locate residential gardens, residential stand-alone houses were extracted from a vector-dataset of buildings. A buffer zone was created around the residential houses, and the buffer was then rasterized, to indicate residential gardens. The model reclassified specific land cover and land use to a scale of 1–10, indicating how suitable the different land uses, and land covers are as oviposition sites for mosquitoes. Suitable land use areas are, e.g., cemeteries, allotment gardens and residential gardens, whereas less suitable are, e.g., airports and motor racetracks. Suitable land covers areas are, e.g., deciduous forests on wetland, and less suitable are, e.g., roads, open water, and impervious surfaces. The reclassified land use and land covers were added together, and then divided by 2 to get a joint metric for land cover and land use. The model also

Table 3 The input data for the oviposition model and their application

Data	Application
<i>NMD Land Cover</i>	Locate suitable land cover (e.g., vegetation)
<i>Digital Surface Model (DSM)</i>	Locate flat roofs
<i>Buildings</i>	Locate residential gardens and flat roofs
<i>Land use vector</i>	Locate industrial areas
<i>NMD Land use</i>	Locate suitable land use (e.g., cemeteries, allotment gardens)
<i>Intra Urban Heat Island (IUHI)</i>	Locate relatively warmer areas

reclassified the IUHI-values to a scale 1–10, where relatively warmer areas were given higher values. The complete reclassifications of land cover, land use and IUHI can be found in Stålnacke (2021) or in the code repository for the model.

Heatmap (Kernel Density Estimation) model

The heatmap algorithm in QGIS (Heatmap (Kernel Density Estimation)) creates a density raster of an input point vector layer using kernel density estimation. Heatmaps allow easy identification of hotspots and clustering of points and is not, despite its name, related to urban warming. The heatmap model used the output from the oviposition WMCA (described in section [Weighted multi criteria analysis \(WMCA\)](#)) to create a heatmap of favorable oviposition sites in Uppsala. The heatmap was used as input in the adult WMCA, as adult mosquitoes are likely to be present in larger numbers in areas that are in proximity to suitable oviposition sites. The raster pixels were turned into vector points, and then a heatmap-algorithm was performed with a maximum distance value of 400 m. Higher oviposition-WMCA values were given a higher weight, as higher oviposition WMCA-values were indicative of higher suitability for oviposition.

Adult model

The adult model make use of several spatial inputs, with each one being an indicator for mosquito suitability in some

way. The input data of the adult model and their application can be seen in Table 4.

The data layers were reclassified to a scale between 1 and 10, based on estimated suitability for prevalence of adult mosquitoes. However, not all outputs utilized the entire scale. The complete reclassifications for each dataset can be seen in Stålnacke (2021, Appendix 2) or in the computer code for the model (Lindberg and Stålnacke 2023).

The vector land use dataset was reclassified and rasterized. More suitable areas were, e.g., urban woodlands. Less suitable areas were, e.g., densely built-up areas. The heatmap (the output from the heatmap model) was reclassified, using an equal interval reclassification. Higher heatmap-values were given higher reclassification-values as adult mosquitoes are likely more prevalent in areas in proximity to their birthplace. Pixels containing vegetation were extracted from the NMD land cover-data, which was then joined with the merged object height-rasters to obtain the heights of the vegetation. This layer was then reclassified. In general, lower vegetation was given higher reclassified values and higher vegetation was given lower reclassified values as *Cx. pipiens* seldom occupy very tall trees. For the NMD land cover, higher reclassified values were given to, e.g., vegetated areas, lower reclassified values were given to, e.g., roads, water, and impervious surfaces.

NMD land cover was used to find ocean pixels. The ocean pixels were used to calculate distance from ocean, which was used to calculate the wind reduction by increasing distance from the ocean by the Eq. (6):

Table 4 The input data for the adult model and their application

Data	Application
<i>Land Cover vector</i>	Locate suitable land covers (e.g., areas with low houses)
<i>Heatmap</i>	Locate oviposition areas
<i>NMD Land Cover</i>	Locate suitable land cover (e.g., vegetation)
<i>NMD Object heights 0.5–5 m</i>	Locate suitable vegetation heights
<i>NMD Object heights 5–45 m</i>	Locate suitable vegetation heights
<i>Leaf Area Index</i>	Locate highly vegetated areas
<i>Morphological grid</i>	Locate morphologically suitable areas
<i>Digital Elevation Model (DEM)</i>	Locate less wind affected areas

$$\text{Wind speed} = u_{ref} * e^{0.015 * dist} \quad (6)$$

where u_{ref} is the wind speed at a reference point (2.4 is chosen here, which is the mean wind speed for Uppsala) and $dist$ is the distance in kilometers from the ocean (Holmer 1985). The wind reduction by increased distance from the ocean was reclassified (0 to 10), so that lower wind speeds (further from the ocean) were given higher reclassified values and vice versa.

The DEM was used together with the morphological grid to get the mean altitude of the grid cells. The mean altitude was used to calculate how the wind speed is affected by altitude, using the wind power law, via the equation below (7):

$$u = u_r \left(\frac{z}{z_r} \right)^a \quad (7)$$

where u is the wind speed at height z , u_r is the known wind speed at the reference height z_r , and a is the power exponent. u was set to 2.6 representing the mean wind speed in Uppsala at 2 m above ground (reference height). a was given the value 0.2 (Givoni 1998). The morphological grid contains the $\lambda_{p\text{veg}}$, which was used as an indicator for bird-rich areas. As the *Cx. pipiens* is ornithophilic, they will likely look for bloodmeals in areas with a higher number of birds. A higher degree of canopy (or vegetation) cover has been found to be an indicator for higher species richness, as well as higher number of individual birds (Hedblom and Söderström 2010). The $\lambda_{p\text{veg}}$ was reclassified, where higher $\lambda_{p\text{veg}}$ -values are given higher reclassified values and vice versa.

The *Cx. pipiens*, like other mosquitoes, are affected by wind patterns in their movement, and are less likely to be found in areas with strong winds. The morphological grid contains the parameter Frontal Area Index (λ_f) of both vegetation ($\lambda_{f\text{veg}}$) and buildings ($\lambda_{f\text{buildings}}$). λ_f is a metric which indicates the area of building walls, or tree trunks, facing a specific wind direction relative to total ground area (Wong and Nichol 2013). Higher values of λ_f indicate areas where wind speeds are reduced due to interference of buildings or vegetation (ibid). The Leaf Area Index (LAI) is also an indicator of wind reduction from vegetation; however, a porosity value must first be added to the LAI. The foliage state of vegetation affects the porosity (and therefore the wind reduction) of the vegetation (Kent et al. 2017). More foliage gives lower porosity and vice versa. The equation for merging LAI, $\lambda_{f\text{veg}}$ and $\lambda_{f\text{buildings}}$ can be seen below (8).

$$\text{Wind reduction} = \frac{[\lambda_{f\text{veg}}(\text{LAI} * \text{porosity}) + \lambda_{f\text{buildings}}]}{2} \quad (8)$$

LAI porosity was set to 0.6. In their search for suitable areas to inhabit, *Cx. pipiens* often look for vegetated areas which provide both shade and a higher humidity than non-vegetated areas. As an indicator for shade and humidity, LAI was used (Andersson-Sköld et al. 2018). The LAI-data was reclassified, where higher LAI-values are given a higher reclassified value.

Weighted multi criteria analysis (WMCA)

A Weighted Multi Criteria Analysis (WMCA) was used to combine the different reclassified datasets to locate areas in Uppsala with relatively higher and lower suitability for the *Cx. pipiens*, both regarding oviposition and adult distribution. The WMCA for oviposition sites only had two inputs, namely the IUHI-raster and the combined land use and land cover raster layer. The weights of the two raster layers were 0.9 and 0.1, respectively. The reasoning for the weighting was that the *Cx. pipiens* are highly adapted to finding oviposition sites all over an urban area and are therefore not strongly affected by air temperature variations in the city. Therefore, the IUHI-layer was not seen as a decisive parameter, but rather as an indicator for areas where mosquito development may be accelerated due to relatively warmer air temperatures.

The input data for the adult WMCA and their weights can be seen in Table 5. All raster layers used in the WMCA were of importance however, not all parameters were given equally importance. In general, the weights were distributed to give higher weights to well-known and strong indicators (e.g., LAI) and to parameters that will affect mosquito distribution more efficiently (e.g., heatmap and ocean-altitude wind patterns). Subsequently, lower weights were given to parameters that are believed to be important, but not as important as the other parameters. LAI had the highest weight due to the metric being a strong indicator for shade and humidity. The heatmap was given the highest weight, as *Cx. pipiens* are not believed to fly far away from their birthplace. The land use had medium-high weight due to the parameter being useful in demarcating suitable land uses from unsuitable. The ocean-altitude wind patterns had medium-high weight, due to wind influencing mosquito distribution. $\lambda_{p\text{veg}}$ was given medium-high weight, as the *Cx. pipiens* are more likely to inhabit bird-rich areas. The vegetation height had medium-low weight, as the level of influence of vegetation heights on the distribution of *Cx.*

Table 5 The weights provided to the raster layers used in the WMCA for adult distribution

Raster	Weight
LAI	0.18
Heatmap (oviposition)	0.18
Land use	0.13
Ocean-altitude wind patterns	0.13
$\lambda_{p\text{veg}}$	0.13
Vegetation heights	0.1
Merged LAI, $\lambda_{f\text{veg}}$ and $\lambda_{f\text{buildings}}$	0.1
NMD Land cover	0.05

Sum of all weights = 1

pipiens is not fully understood. Medium–low weight was given to the merged LAI, $\lambda_{f\text{veg}}$ and $\lambda_{f\text{buildings}}$ as the wind reduction from vegetation is already partially given in the LAI-parameter. So, to avoid an overrepresentation of vegetation-parameters, the merged LAI, $\lambda_{f\text{veg}}$ and $\lambda_{f\text{buildings}}$ -parameter was given lower weight. NMD Land cover had low weight as the parameter was mostly used to mask away unsuitable areas (e.g., roads and water).

Results

Observations of mosquito prevalence and local climate

All in all, 452 specimens of 10 species were trapped throughout the field campaign (Table 6). The most common was female *Culex pipiens*, accounting for 69.5% of the total number of trapped mosquitoes.

The population numbers of trapped mosquitoes—foremost *Culex (Cx) pipiens*—are increasing from spring up late summer and then decreasing as females are not taking any more bloodmeals late in the season to prepare for the winter (Fig. 3a). The general summer weather in Uppsala, 2022, is represented by daily air temperature and precipitation, as officially provided for the associated meteorological station from SMHI and shown in Fig. 3b. The numbers of mosquitoes trapped vary substantially depending on location within the city. The two sites where most mosquitoes were trapped are the botanical garden and the allotment gardens. The residential (detached houses) area also shows relatively high number of trapped animals. The more urbanised sites (industry, city centre, mixed city) show the lowest number of mosquitoes trapped throughout the season. Surprisingly, a low number of mosquitoes was caught in

the graveyard. This is further discussed in the Discussion section. No clear relationships are found between ambient air temperature and humidity over time and number of mosquitoes trapped (not shown).

When comparing the air temperature difference between the different site locations and the standard meteorological site (SMHI) it is shown that the air temperature increases with building volume fraction (Fig. 4a) i.e., the denser the more intense intra urban heat island (IUHI). This urban heat island effect is a well-known phenomenon and shown before in Uppsala by pioneering work made by Sundborg (1951). However, no relationship ($R^2 = 0.02$) is found between the IHUI and total number of captured mosquitoes (not shown). There is also a clear relationship, but not significant ($p > 0.05$), between green factor and number of mosquitos captured. When comparing the humidity difference between the different site locations and the standard meteorological station, it is shown that the air humidity increases with higher green fraction (Fig. 4b, here represented by trees and grass (see Fig. 1). A significant linear relationship (excluding the graveyard location) between number of trapped mosquitoes and specific humidity is found (Fig. 4d), where the number of mosquitoes increases with increased air humidity ($p < 0.05$). This implies that mosquito prevalence is connected to intra-urban humidity differences developed from differences in urban greening, but not to intra-urban temperature differences. No covariation between humidity and temperature were found (not shown).

Model results and evaluation

The oviposition map i.e., potential attractive areas for mosquitos to lay their eggs, show large intra-urban variations (Fig. 5, left), with gardens and parks being most attractive and impervious surfaces and flatlands being least attractive. No clear urban effect, i.e., urban–rural differences is found. The adult map, i.e., potential attractive areas for mosquitos (Fig. 5, right), however show a clear urban effect with the central densely built-up areas having lower attractiveness than surrounding landscapes (e.g., forests, and gardens). Green areas within the urban areas, such as gardens and parks form islands of higher attractiveness for mosquitos.

The raw-value heatmap generated from the oviposition WMCA map in Fig. 5 (left) is shown in Fig. 6. Blue areas (high values) indicate areas more favourable sites for oviposition. This map is later linearly reclassified between 1 and 10 before it is used in the adult WMCA creating the final output of the model. The central parts of the heatmap show the lowest values meaning that these parts of Uppsala is where the lowest number of mosquitos are hatched based on the model presented here. As shown in

Table 6 Species and specimens captured in the field campaign 2022 Uppsala, Sweden

Species	Number of specimens	%
<i>Culex pipiens</i>	314	69.5
<i>Culex torrentium</i>	71	15.7
<i>Aedes cantans</i>	22	4.9
<i>Coquillettidia richiardii</i>	21	4.6
<i>Aedes cinereus</i>	11	2.4
<i>Culiseta morsitans</i>	5	1.1
<i>Aedes vexans</i>	4	0.9
<i>Aedes punctator</i>	2	0.4
<i>Anopheles maculipennis s.l</i>	1	0.2
<i>Aedes sticticus</i>	1	0.2
Total	452	100.0

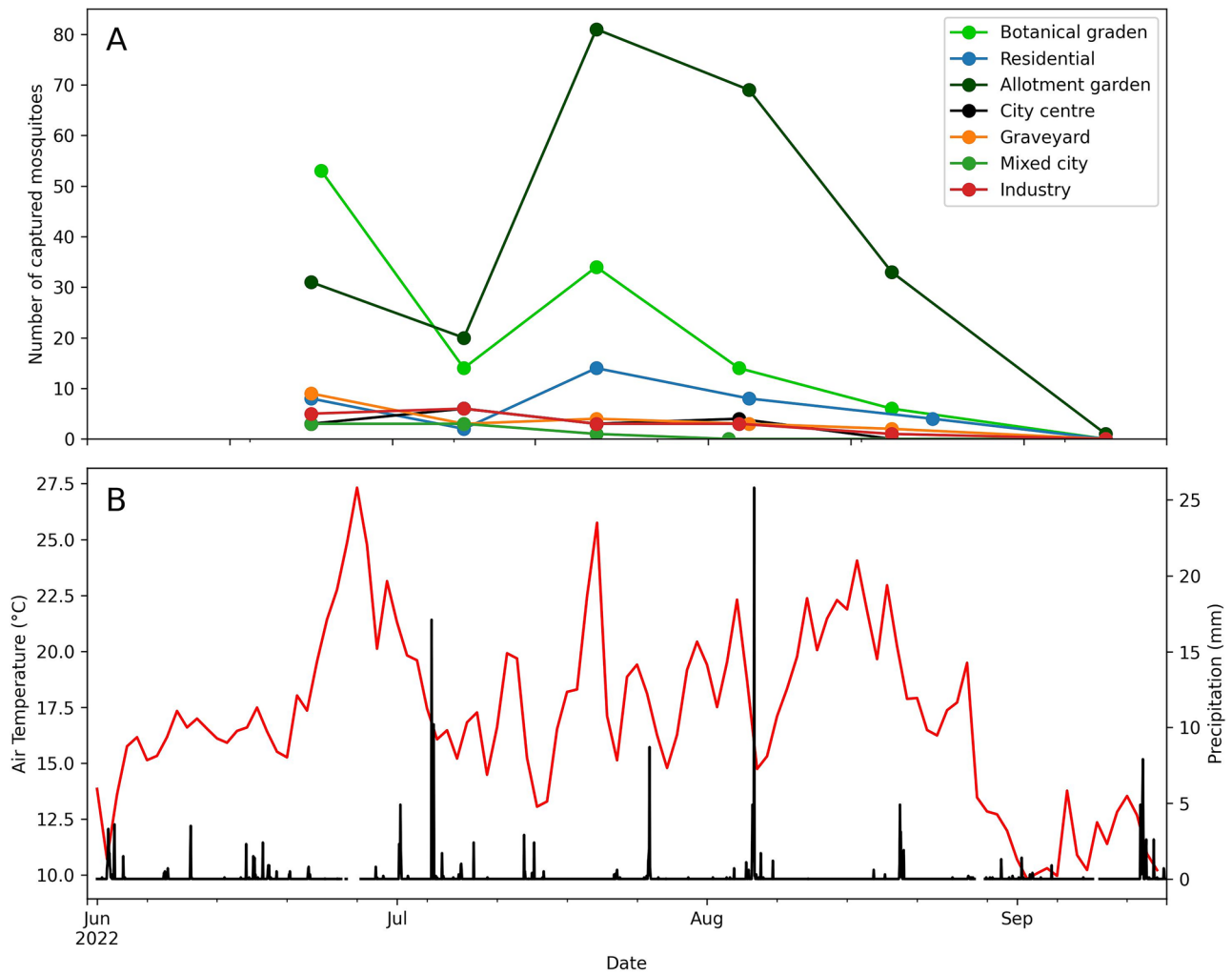


Fig. 3 **A** Number of mosquitoes captured at seven locations from late June to early September 2023. **B** Air temperature and precipitation from meteorological station 97510 (of the Swedish Meteorological and Hydrological Institute (SMHI)) during the observation period summer 2023

Tab. 5, the heatmap in Fig. 6 has the weight 0.18 which means that the oviposition heatmap only contributes by 18% of the final spatial pattern as shown in Fig. 5 (right).

The model shows an overall good agreement ($R^2 = 0.66$, $p < 0.05$) with the observations (Fig. 7). The model output can theoretically vary between 1 and 10 based on the WMCA, where high values are locations with predicted high prevalence of mosquitoes. The allotment garden show the highest predicted prevalence, followed by the graveyard, the botanical garden and the residential area, whereas densely built-up areas (mixed city, city centre and industry) show the least predicted prevalence, which is consistency with the numbers of captured mosquitoes, except for the graveyard where the model predict higher prevalence of mosquitoes than observed.

Discussion

Observation of mosquito prevalence

In this study the prevalence and distribution, of mosquitoes within the urban area of Uppsala during the Summer of 2022 is quantified, both in time as well as space. As shown in Fig. 3, the total population grows up until late July early August and then gradually decline as seen in other studies (Spielman 2001). The summer of 2022 was close to a normal summer where levels of precipitation and temperature were around the climatological average for the Uppsala region. There is a clear spatial pattern where sites that can be considered as more urban, i.e., have higher building compactness, more impervious surfaces and less

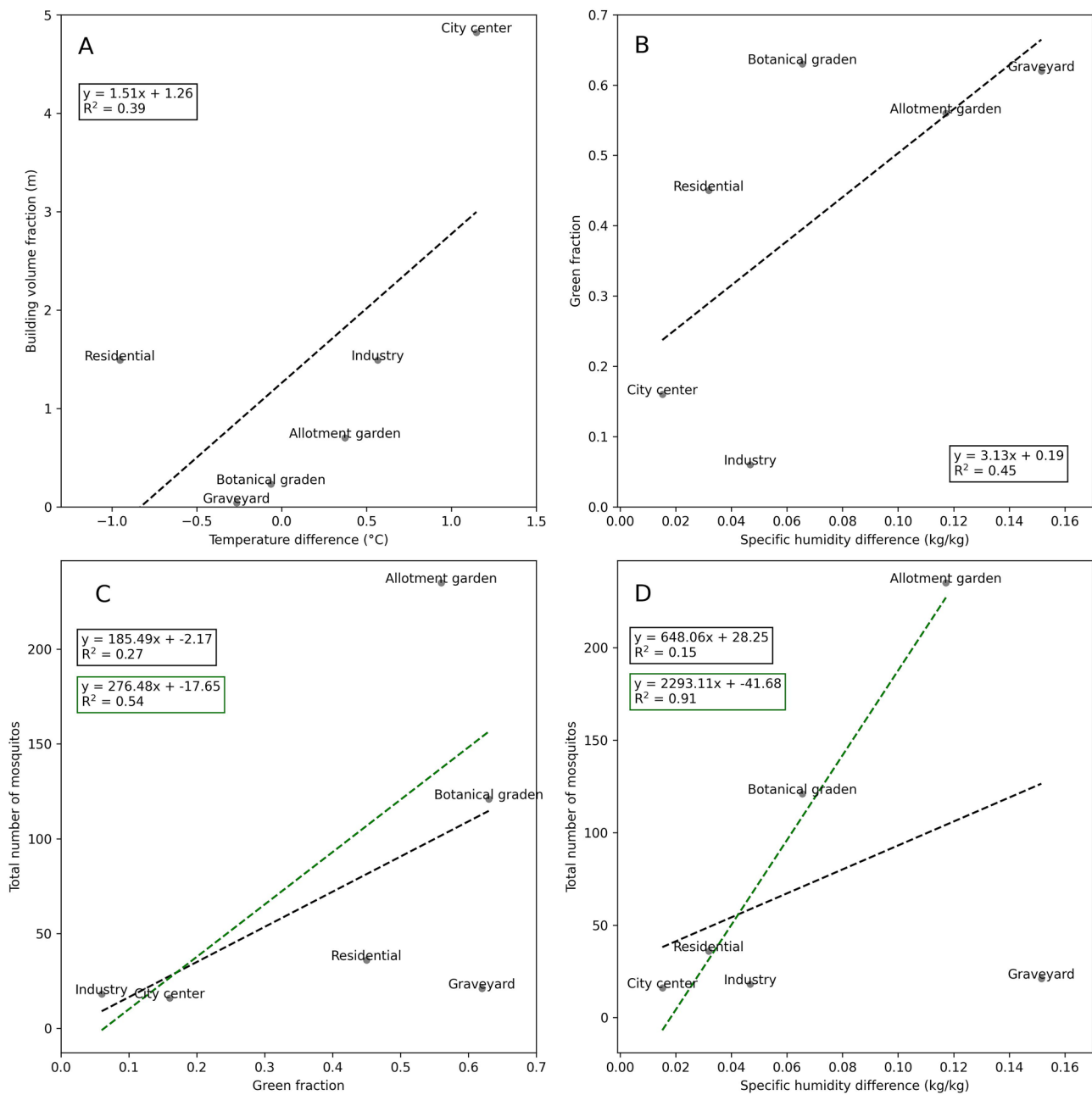


Fig. 4 Scatterplots and linear fits of **A** building volume fraction versus average urban rural temperature difference from the standard meteorological site (of the Swedish Meteorological and Hydrological Institute (SMHI)), **B** green fraction (grass and trees) versus urban rural humidity difference from the standard meteorological

site (of SMHI, station no. 97510), and total number of mosquitoes captured versus average difference in the capture sites from the standard meteorological site (of SMHI) for **C** green fraction, and **D** specific humidity. The green line and textbox show the linear fit if the Graveyard site is excluded

green, have lower prevalence of mosquitoes throughout the Summer. In contrast, a higher green-area fraction, such as in the allotment area and the botanical garden, have the highest prevalence of mosquitoes trapped in this study. The temporal and spatial patterns also follow each other, i.e., the variation in time does not change the intra-urban spatial pattern of mosquito prevalence. High positive

correlation is found between the prevalence of adult mosquitoes and specific relative humidity (Fig. 4d, $R^2 = 0.91$, $p < 0.05$), if the anomalous graveyard site is excluded. A relatively high correlation is also found between green-area fraction and specific humidity (Fig. 4b, $R^2 = 0.45$) indicating that the green-area fraction variable can be used as a proxy for mosquito prevalence in urban areas.

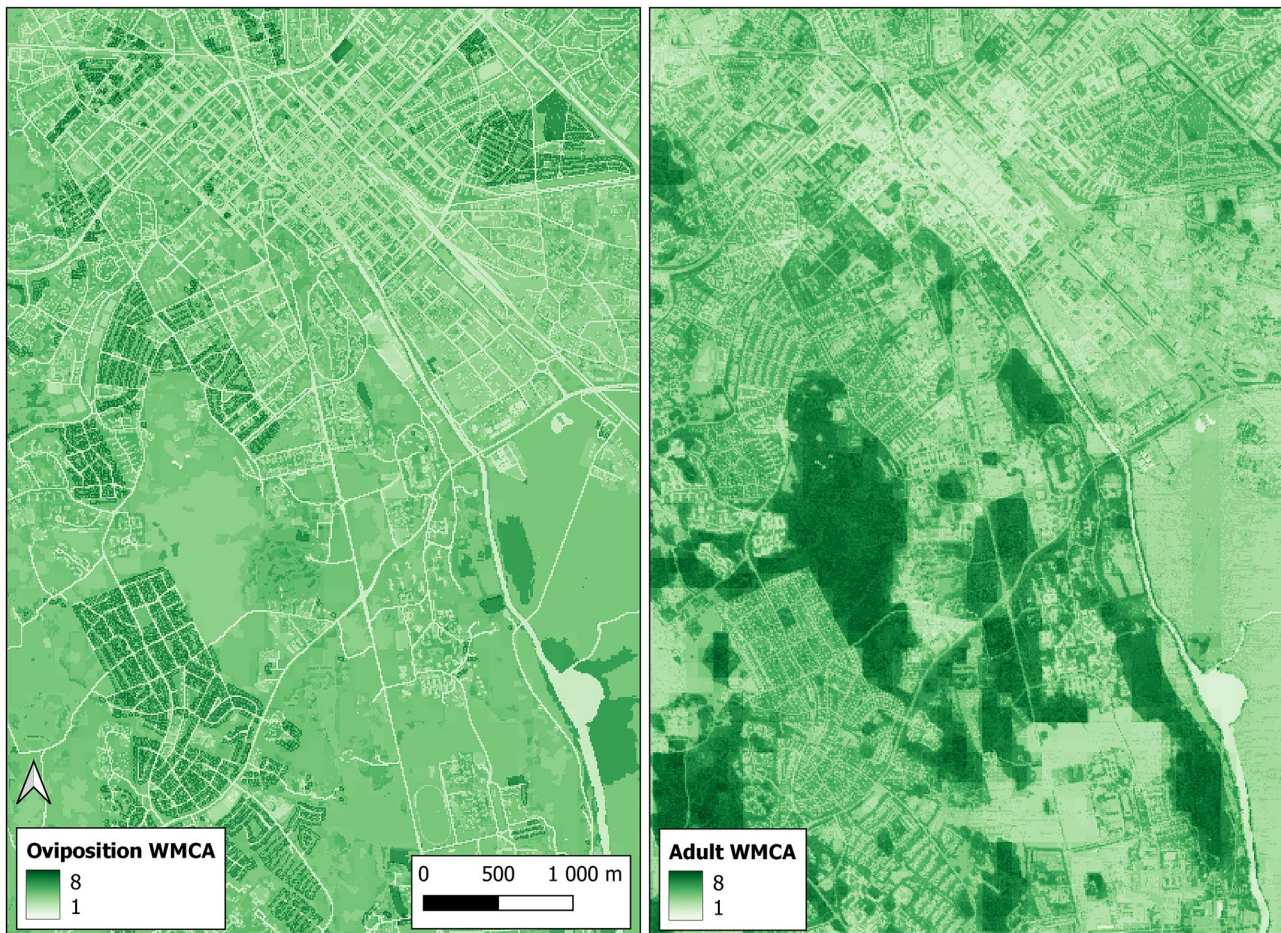


Fig. 5 Output from the UMP model developed in this study. Left: Oviposition WMCA. Right: Final adult WMCA. The scales in both legends show the model score where higher numbers are more attrac-

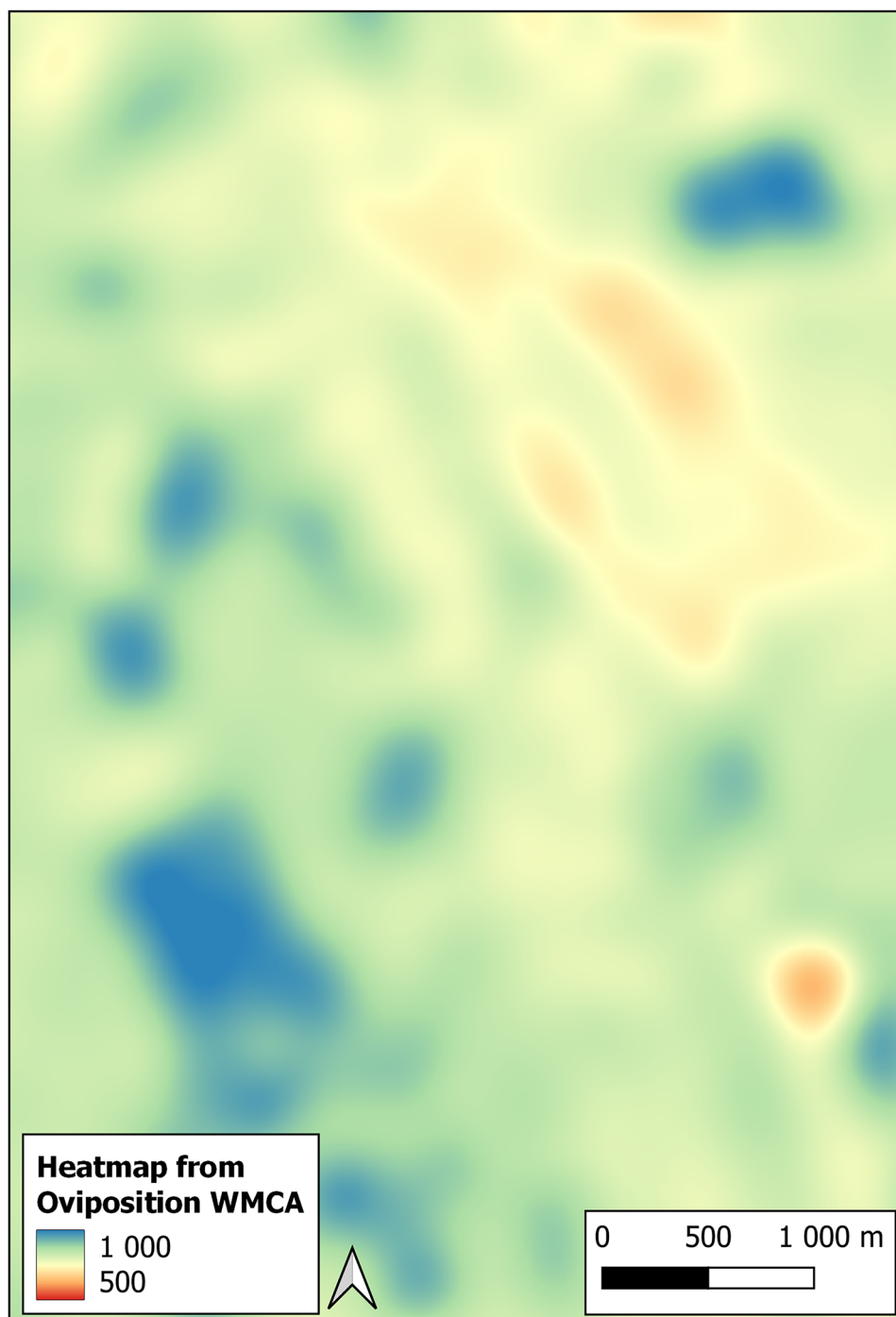
tive locations for oviposition and adult presence, respectively. Pixel resolution is 10 m

As mentioned, the graveyard result is anomalous compared to the general pattern found in this study, in that it has a high green-area fraction and a low building volume fraction but still does not have a high number of trapped mosquitoes (Fig. 4). A reason for this could be that this site includes mature and high trees with a relatively low fraction of low vegetation. This is exemplified in Table 1, with the graveyard having the highest mean tree height. As *Cx. pipiens*, which is the dominating captured species, prefer birds for their blood meal, it could be so that the majority of the mosquito population did not prevail on the ground, where the trap was located, but higher up in the tree crowns, along with the majority of the bird population. A previous study by Hutchinson et al. (2007) has shown that significantly more *Cx. pipiens* s.l. were trapped at 5 m height compared to 1 or 2,5 m height. Similar results were also found by Russel and Hunter (2010), who trapped significantly more *Cx. pipiens* at 5 m than at 1,5 m. Moreover, L'Ambert et al. (2012) showed that, even though overall more mosquitoes are trapped close

to the ground, for *Cx. pipiens* a larger population fraction is found in tree canopies. The latter finding is also consistent with the earlier study by Anderson et al. (2004), comparing the number of *Cx. pipiens* trapped at ground level to the number trapped in tree canopies, and finding that significantly more *Cx. pipiens* were trapped in the tree canopies. It is therefore plausible that *Cx. pipiens* would mainly be found in the tree canopies of the graveyard site with its high trees and small undergrowth.

The observations in this study were made at seven sites throughout summer with the aim to choose sites that covered a broad spatial variation within the city of Uppsala. Based on some screening observations in the summer of 2021 of more sites and fragrances, we chose to focus the final study on a selection of fewer sites and one fragrance throughout the summer. More sites would have been logistically challenging when also attempting to cover the temporal variations over the summer. Hence, instead of having more sites, the traps were set out many times at the selected seven final sites,

Fig. 6 The heatmap generated from the oviposition WMCA. Pixel resolution is 2 m



providing a better view of the relation between the spatial and temporal variations of mosquito prevalence within the urban environment.

Model performance and evaluation

The correlation between the UMP-model results and observations is high ($R^2=0.66$, $p < 0.05$, omitting the graveyard;

Fig. 7). Even if the graveyard is included the correlation is relatively high ($R^2=0.4$; Fig. 7). The model thus seems to capture most of the spatial pattern and can predict the occurrence of mosquitoes in the studied Swedish city based on commonly available geodata. One model limitation is the absence of a more detailed description of the vertical distribution of vegetation, which could account for the tree canopy favoring of *Cx. pipiens*. Model extension to overcome

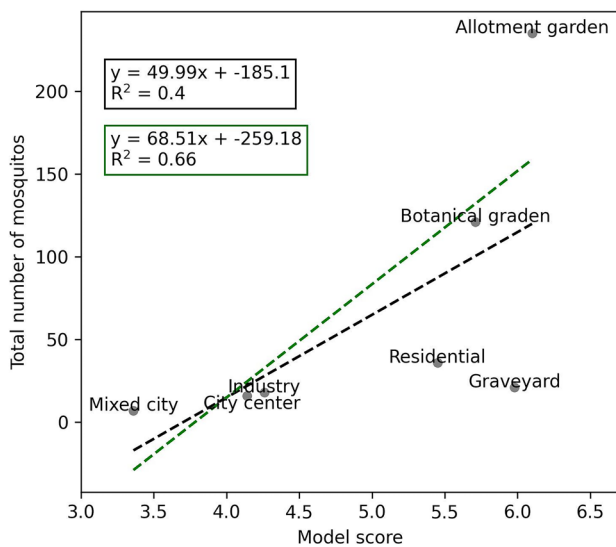


Fig. 7 Scatterplot between total number of mosquitoes captured and model score from MCA-based GIS model presented in the study. The green line and textbox show the linear fit if the Graveyard site is excluded

this limitation could be used to identify areas, such as the graveyard site, with mature, tall trees and sparse lower vegetation (e.g., Lindberg and Grimmond 2011).

The UMP-model developed and tested in this paper relies on open-source tools and open national geodata for Sweden. This makes it readily possible to transfer and replicate the modelling for other cities in Sweden. More detailed proprietary data could be available that could be used to improve model performance. Transferring this model to cities in other parts of the world, outside of Sweden, is also promising since most of the datasets available for Swedish cities are also commonly available for cities in other countries, for example land cover and land use data which are available for cities over both global and regional/national scales (e.g., Goldenberg et al. 2021). One challenge could be to interpret and convert land cover/land use classes as these may differ between datasets.

Overall, this study has demonstrated the importance of green-area fraction (grass and trees) for mosquito prevalence. Thus, it is important to use high quality data that can represent vegetation with high resolution in urban environments. LiDAR data is one such data source, providing the raw data for many of the input layers used in our model (elevation models and LAI), and becoming increasingly available on national level for many counties around the world (Kakoulaki et al. 2021). Here, LiDAR is used to derive LAI from remote sensing techniques. The results of the used LAI model (Klingberg et al. 2017) are to some extent sensitive to how the data was acquired and processed by the vendor. Examining the final adult model in detail

(Fig. 5, right), one can identify some north to south linear features, e.g., in the eastern part of the study area, due to flight overlaps with more returns affecting the LAI-model results. By exploiting the *ThinData*-algorithm in FUSION LDV (McGaughy 2009), reducing the number of returns in these areas, the effect is minor.

As this is a simple linear WMCA model, the weights can be altered if and as more data become available, or if some data sources are unavailable. One of the strengths of this model is its two parts, one for estimating oviposition and the other an adult model providing the final result. We have chosen not to further calibrate model weights and scores based on the actual numbers of captured mosquitoes, but rather use the obtained model results as an indication on the urban spatial distribution of mosquitoes.

Concluding remarks

The Uppsala case study shows that the developed WMCA model can resolve mosquito prevalence variations and their GBI relationships within urban environments. A clear relationship is seen with green-area fraction (grass and trees), indicating that urban GBI extension can enhance mosquito prevalence, with possible negative impacts on infectious disease spreading, along with the important urban GBI benefits. This relationship is also supported directly by data, showing greater mosquito prevalence with higher ambient humidity, which is in turn related to larger green-area fraction. This study also show that intra urban temperature differences has no effect on mosquito prevalence.

The UMP-model ability to satisfactory estimate ($R^2 = 0.66$, $p > 0.05$) spatial mosquito variations within Uppsala based on open data and tools is promising and calls for further research on the possible wider applicability of this modelling approach to various urban conditions. Identification and quantification of urban relationships between mosquito abundance and different GPI features around a city are generally needed, e.g., in urban development planning that needs to account for and seek relevant trade-off balances between positive and negative effects of urban GBI changes. The presented WMCA modelling approach can contribute to such urban accounting capability and has emerged as worthy of further testing for other cities in Sweden and other parts of the world.

Acknowledgements We are grateful to Klara Lindström who helped collect the mosquitoes, Disa Eklöf who identified them morphologically and Tobias Lija who did the molecular work.

Author contributions The study was conceptualized by FL, AL, ST and GD. FL and AL managed the field observations. VS, FL and AL developed the model. Model-data was curated by VS and FL. Data analysis and model evaluation was made by FL. FL and VS wrote

the main manuscript text. FL, AL, ST and GD reviewed and edited the manuscript.

Funding Open access funding provided by University of Gothenburg. Financial support was provided by FORMAS, the Swedish Research Council for Environment, Agricultural Sciences and Spatial Planning (2019-00773).

Data availability The model code and datasets are available from <https://doi.org/10.5281/zenodo.10185523> (Lindberg and Stålnacke 2023). Code is also available from the GitHub repositories below: LiDAR to surface, land cover and LAI datasets: <https://github.com/biglimp/LidarToDSMs>. UMP-model: <https://github.com/biglimp/MosquitoModel>.

Declarations

Ethical approval Not applicable.

Competing interests The authors declare no competing interests.

Open Access This article is licensed under a Creative Commons Attribution 4.0 International License, which permits use, sharing, adaptation, distribution and reproduction in any medium or format, as long as you give appropriate credit to the original author(s) and the source, provide a link to the Creative Commons licence, and indicate if changes were made. The images or other third party material in this article are included in the article's Creative Commons licence, unless indicated otherwise in a credit line to the material. If material is not included in the article's Creative Commons licence and your intended use is not permitted by statutory regulation or exceeds the permitted use, you will need to obtain permission directly from the copyright holder. To view a copy of this licence, visit <http://creativecommons.org/licenses/by/4.0/>.

References

- Åhlen I, Jarsjö J, Hambäck P (2023) Connecting wetland flooding patterns to insect abundance using high-resolution inundation frequency data. *Wetlands* 43:74
- Anderson J, Andreadis T, Main A, Kline D (2004) Prevalence of West Nile virus in tree canopy-inhabiting *Culex pipiens* and associated mosquitoes. *Am J Trop Med Hyg* 71(1):112–119
- Andersson-Sköld Y, Klingberg J, Gunnarsson B, Thorsson S (2018). Metod för bedömning och värdering av ekosystemtjänster i staden (VEKST). Handbok version 1.0. Statens väg och transportforskningsinstitut (VTI) Göteborgs botaniska trädgård Göteborgs universitet, (in Swedish)
- Becker N, Petric D, Zgomba M (2020) Mosquitoes - identification, ecology and control, 3rd edn. Springer, Cham, Switzerland, p 570
- Desvars A, Furberg M, Hjertqvist M, Vidman L, Sjöstedt A, Rydén P, Johansson A (2015) Epidemiology and ecology of tularemia in Sweden, 1984–2012. *Emerg Infect Dis* 21:32–39
- Diuk-Wasser MA, Brown HE, Andreadis TG, Fish D (2006) Modeling the spatial distribution of mosquito vectors for West Nile virus in Connecticut, USA. *Vector-Born Zoonotic Dis* 6:283–295
- Engler O, Savini G, Papa A, Figuerola J, Groschup MH, Kampen H, Medlock J, Vaux A, Wilson A, Werner D, Jöst H, Goffredo M, Capelli G, Federici V, Tonolla M, Patocchi N, Flacio E, Portmann J, Rossi-Pedruzzi A, Mourelatos S, Ruiz S, Vazquez A, Calzolari M, Bonilauri P, Dottori M, Schaffner F, Mathis A, Johnson N (2013) European surveillance for West Nile virus in mosquito populations. *Int J Environ Res Public Health* 10(10):4869–4895
- Ferraguti M, Martínez-de la Puente J, Roiz D, Ruiz S, Soriguer R, Figuerola J (2016) Effects of landscape anthropization on mosquito community composition and abundance. *Sci Rep* 6:29002
- Frank C, Schmidt-Chanasi J, Ziegler U, Lachmann R, Preussel K, Offergeld R (2022) West Nile virus in Germany: An emerging infection and its relevance for transfusion safety. *Transfus Med Hemotherapy* 49:192–203
- Givoni B (1998) Climate considerations in building and urban design. Van Nostrand Reinhold, the USA
- Goldenberg R, Kalantari Z, Cvetkovic V, Mörtberg U, Deal B, Destouni G (2017) Distinction, quantification and mapping of potential and realized supply-demand of flow-dependent ecosystem services. *Sci Total Environ* 593–594:509–609
- Goldenberg R, Kalantari Z, Destouni G (2018) Increased access to nearby green–blue areas associated with greater metropolitan population wellbeing. *Land Degrad Dev* 29:3607–3616
- Goldenberg R, Kalantari Z, Destouni G (2021) Comparative quantification of local climate regulation by green and blue urban areas in cities across Europe. *Sci Rep* 11:23872
- Hedblom M, Söderström B (2010) Landscape effects on birds in urban woodlands: An analysis of 34 Swedish cities. *J Biogeogr* 37(7):1302–1316
- Holmer B (1985) Energi-index: lokalklimatets påverkan på energiförbrukningen (in Swedish). LiberTryck, Stockholm
- Hutchinson R, West P, Lindsay S (2007) Suitability of two carbon dioxide-baited traps for mosquito surveillance in the United Kingdom. *Bull Entomol Res* 97:591–597
- Jourdain F, Roiz D, de Valk H, Noël H, L'Ambert G, Franke F, Paty M-C, Guinard A, Desenclos J-C, Roche B (2020) From importation to autochthonous transmission: Drivers of chikungunya and dengue emergence in a temperate area. *PLoS Negl Trop Dis* 14(5):e0008320
- Kakoulaki G, Martinez A, Florio P (2021) Non-commercial Light Detection and Ranging (LiDAR) data in Europe. *JCR Tech Rep*. https://publications.jrc.ec.europa.eu/repository/bitstream/JRC126223/jrc126223_jrc126223_lidaropensourcedata.pdf. Accessed 29 June 2023
- Kent CW, Grimmond S, Gatey D (2017) Aerodynamic roughness parameters in cities: Inclusion of vegetation. *J Wind Eng Ind Aerodyn* 169:168–176
- Klingberg J, Konarska J, Lindberg F, Johansson L, Thorsson S (2017) Mapping leaf area of urban greenery using aerial LiDAR and ground-based measurements in Gothenburg, Sweden. *Urban For Urban Green* 26:31–40. <https://doi.org/10.1016/j.ufug.2017.05.011>
- Konarska J, Uddling J, Holmer B, Lutz M, Lindberg F, Pleijel H, Thorsson S (2016) Transpiration of urban trees and its cooling effect in a high latitude city. *Int J Biometeorol* 60(1):159–172
- Kramer LD, Ciota AT (2015) Dissecting vectorial capacity for mosquito-borne viruses. *Curr Opin Virol* 15:112–118
- Krayenhoff ES, Broadbent AM, Zhao L, Georgescu M, Middel A, Voogt JA, Erell E et al (2021) Cooling hot cities: A systematic and critical review of the numerical modelling literature. *Environ Res Lett*. <https://doi.org/10.1088/1748-9326/abdcd1>
- Krol L, Blom R, Dellar M, van der Beek JG, Stroo ACJ, van Bodegom PM et al (2023) Interactive effects of climate, land use and soil type on *Culex pipiens/torrentium* abundance. *One Health* 17:100589
- Krüger A, Börstler J, Badusche M, Lühken R, Garms R, Tannich E (2014) Mosquitoes (Diptera: Culicidae) of metropolitan Hamburg, Germany. *Parasitol Res*. <https://doi.org/10.1007/s00436-014-3952-3>

- L'Ambert G, Ferré J-B, Schaffner F, Fontenille D (2012) Comparison of different trapping methods for surveillance of mosquito vectors of West Nile virus in Rhône Delta, France. *J Vector Ecol* 37(2):269–275
- Lantmäteriet (2021) Swedish mapping cadastral and land registration authority. Geodataportalen. <https://www.geodata.se/geodataportalen/>. Retrieved 21 Jan 2021
- Lantmäteriet (2023) Laser data Download, forest. https://www.lantmateriet.se/globalassets/geodata/geodataprodukter/hojddata/pb_laserdata_nedladdning_skog.pdf. Accessed 18 Apr 2023
- Lindberg F, Grimmond CSB, Gabey A, Huang B, Kent CW, Sun T, Theeuwes N, Järvi L, Ward H, Capel-Timms I, Chang YY, Jonsson P, Krave N, Liu D, Meyer D, Olofson F, Tan JG, Wästberg D, Xue L, Zhang Z (2018) Urban Multi-scale Environmental Predictor (UMEP): An integrated tool for city-based climate services. *Environ Model Softw* 99:70–87
- Lindberg F, Grimmond S (2011) Nature of vegetation and building morphology characteristics across a city: Influence on shadow patterns and mean radiant temperatures in London. *Urban Ecosyst* 14(4):617–634
- Lindberg F, Grimmond S, Martilli A (2015) Sunlit fractions on urban facets – Impact of spatial resolution and approach. *Urban Clim* 12:65–84
- Lindberg F, Stålnacke V (2023) Urban mosquito prevalence model and test datasets (1.0). Zenodo. <https://doi.org/10.5281/zenodo.10185523>
- Lindström A, Eklöf D (2022) Stickmyggor i Nordeuropa - en fälthandbok. Entomologiska Föreningen i Stockholm (in Swedish)
- Lundström JO, Schäfer ML, Hesson JC, Blomgren E, Lindström A, Wahlqvist P, Halling A, Hagelin A, Ahlm C, Evander M, Broman T, Forsman M, Persson Vinnersten TZ (2013) The geographic distribution of mosquito species in Sweden. *J Eur Mosq Control Assoc* 31:21–35
- Ma Y, Bring A, Kalantari Z, Destouni G (2019) Potential for hydroclimatically driven shifts in infectious disease outbreaks: The Case of Tularemia in high-latitude regions. *Int J Environ Res Public Health* 16:3717
- Ma Y, Vigouroux G, Kalantari Z, Goldenberg R, Destouni G (2020) Implications of projected hydroclimatic change for Tularemia outbreaks in high-risk areas across Sweden. *Int J Environ Res Public Health* 17:6786
- McGaughey RJ (2009) FUSION/LDV: Software for LiDAR data analysis and visualization. United States Department of Agriculture, Seattle
- Medlock JM, Hansford KM, Anderson M, Mayho R, Snow KR (2012) Mosquito nuisance and control in the UK – A questionnaire-based survey of local authorities. *Eur Mosq Bull* 30:15–29
- Oke TR (2002) Boundary layer climates. Routledge, boundary layer climates. <https://doi.org/10.4324/9780203407219>
- Paz S, Albersheim I (2008) Influence of warming tendency on *Culex pipiens* population abundance and on the probability of West Nile fever outbreaks (Israeli Case Study: 2001–2005). *EcoHealth* 5:40
- Petrić M, Lalić B, Ducheyne E, Djurdjević V, Petrić D (2017) Modelling the regional impact of climate change on the suitability of the establishment of the Asian tiger mosquito (*Aedes albopictus*) in Serbia. *Clim Change* 142(3–4):361–374
- Public Health Agency of Sweden (2019) Sjukdomsinformation om West Nile-virusinfektion. <https://www.folkhalsomyndigheten.se/smittskydd-beredskap/smittsamma-sjukdomar/west-nile-fever-wnf/>
- QGIS.org (2023) QGIS 3.28. Geographic Information System API Documentation. QGIS Association. Electronic document: <https://qgis.org/pyqgis/3.28/index.html>
- Reisen WK, Meyer RP, Tempelis CH, Spoehel JJ (1990) Mosquito abundance and bionomics in residential communities in Orange and Los Angeles counties, California. *J Med Entomol* 27:356–367
- Roiz D, Ruiz S, Soriguer R, Figuerola J (2015) Landscape effects on the presence, abundance and diversity of mosquitoes in Mediterranean wetlands. *PLoS One* 10:e0128112
- Rudolf M, Czajka C, Börstler J, Melaun C, Jöst H, von Thien H, Badusche M, Becker N, Schmidt-Chansit J, Krüger A, Tannich E, Becker S (2013) First nationwide surveillance of *Culex pipiens* complex and *Culex torrentium* mosquitoes demonstrated the presence of *Culex pipiens* biotype *pipiens/molestus* hybrids in Germany. *PLoS One* 8(9):e71832
- Russel C, Hunter F (2010) Influence of elevation and avian or mammalian hosts on attraction of *Culex pipiens* (Diptera: Culicidae) in southern Ontario. *Can Entomol* 142:250–325
- Spielman A (2001) Structure and seasonality of Nearctic *Culex pipiens* populations. *Ann N Y Acad Sci* 951(1):220–234
- Stålnacke V (2021) Modelling mosquito prevalence on a City-scale in Gothenburg, Sweden. A methodological development study. Master Thesis, B1128, Department of Earth Sciences, University of Gothenburg, Sweden
- Sundborg Å (1951) Climatological Studies in Uppsala. Geographica No 22, Department of Meteorology, Uppsala University, Sweden
- Swedish Environmental Protection Agency (2020) Nationella Marktäckedata (NMD). <https://www.naturvardsverket.se/>. Retrieved 22 Jan 2021
- Verstiert V, Boyer S, Damiens D, De Clercq EM, Dekonick W, Ducheyne E, Grootaert P, Garros C, Hance T, Hendrickx G, Coosemans M, Van Bortel W (2013) Nationwide inventory of mosquito biodiversity (Diptera: Culicidae) in Belgium. *Europe Bull Entomol Res* 103:193–203
- Vlaskamp D, Thijsen S, Reimerink J, Hilken P, Bouvy W, Bantjes S, Vlamincx B, Zaaijer H, van den Kerkhof H, Raven S, Reusken C (2020) First autochthonous human West Nile virus infections in the Netherlands, July to August 2020. *Eurosurveillance* 25(46):1–4
- Vogels C, van de Peppel L, van Vliet A, Westenbergh M, Ibañez-Justicia A, Stroo A, Buijs J, Visser T, Koenraadt C (2015) Winter activity and aboveground hybridization between the two biotypes of the West Nile virus vector *Culex pipiens*. *Vector-Borne Zoonotic Dis* 15(10):1–8
- Wong MS, Nichol JE (2013) Spatial variability of frontal area index and its relationship with urban heat island intensity. *Int J Remote Sens* 34(3):885–896